

UNIVERSITY OF MILANO-BICOCCA
Department of Physics
"G. Occhialini"



SUPERMASSIVE BINARY BLACK HOLES AND THEIR DYNAMICS IN GALACTIC NUCLEI

Supervisor: MONICA COLPI

Candidate: ULYANA DUPLETSA
776124

Academic Year
2015-2016

To someone

Contents

1	Overview	1
1.1	Outline of the project	2
2	Introducing black holes	3
2.1	Black holes classification and interaction	3
2.2	Binary black holes merger rate and their detection	5
3	Observational evidence for interacting black holes	7
3.1	Direct observations	7
3.2	Indirect observations	8
4	Phases of coalescence	10
4.1	Phase I	10
4.2	Phase II	12
4.3	Phase III	12
5	Final parsec problem	15
6	Setting the galaxy model	17
6.1	Dehnen profile	17
6.1.1	Circular velocity and velocity dispersion	18
7	Black hole - host galaxy correlations	21
7.1	$M_{\bullet} - \sigma$ and $M_{\bullet} - M_{*}$ relations	21
7.2	Morphology of elliptic and spiral galaxies	22
8	Estimates of coalescence time	23
8.1	Plots of coalescence times	25
8.2	Stellar density in elliptical galaxies and in bulges of spirals	27
9	Conclusions	29

Abstract

Super-Massive Black Holes (SMBHs) are hosted at the centre of galaxies and are correlated with their host very tightly, suggesting a symbiotic evolution between them. Galaxy mergers are responsible for bringing them close enough, due to dynamical friction, to form a gravitationally bound system, i.e. a Super-Massive Black Hole Binary (SMBHB). After a phase of interactions with stars, the binary evolution can end with the gravitational wave emission and coalescence.

The aim of this project is to investigate whether such systems are able to coalesce in less than the Hubble time. If so, such binaries would be a promising source of gravitational waves for space gravitational wave detectors (such as the forthcoming LISA). However, the binary may stall at a separation of 1 parsec. This stalling problem is due to the lack of low angular momentum stars with which to interact and is commonly referred to as the *Final Parsec Problem*. It can be overcome if one lets drop the hypothesis of spherical symmetry of the models, since, in reality, the galaxy merger remnant is not spherically symmetric.

The problem will be studied modeling the galaxy with a Dehnen profile and following the work of Sesana and Khan.

Chapter 1

Overview

Black holes are predicted by Einstein's theory of General Relativity. Indirect astronomical observations show that black holes exist in two mass ranges: stellar black holes present in every galaxy and supermassive black holes residing at the centre of galaxies.

The presence of a supermassive black hole at the centre of a galaxy has tight correlations with its stellar population. $M_{\bullet} - \sigma$ relation correlates the stellar velocity dispersion with the black hole mass. Similarly there is a correlation between the mass of the galaxy and the mass of the black hole ($M_{\bullet} - M_{*}$ relation), suggesting that there exists a symbiotic evolution between the black hole and its host galaxy.

In the paradigm of Λ Cold Dark Matter (Λ -CDM) cosmology, galaxies form through hierarchical merging. If both galaxies contain a supermassive black hole at their centres, then the two black holes will form a binary system. Astronomical observations reveal the existence of pairs of black holes in interacting galaxies at distances of few kpc.

The evolution of the two black holes, after the merger of their galaxies, consists of three phases.

In *phase I* dynamical friction is responsible for the black holes sinking to the centre of the system. Dynamical friction can be seen as the drag induced on the massive body, the black hole in our case, by the stellar over-density the massive body itself induces. Stars moving slower than the massive body cause its progressive sinking towards the centre. Dynamical friction stops contributing to the inspiraling motion of the two black holes when the mass in stars enclosed in their orbit is comparable to the mass of the two black holes. Under these conditions, the black hole pair forms a Keplerian binary.

Phase II is characterized by interactions between the black hole binary and a field star. The interaction extracts additional energy and angular momentum from the binary, which shrinks its semi-major axis. In order to get the binary at a separation of order of a mpc, it's necessary the presence of a large reservoir of stars characterized by low angular momentum able to interact with the black hole binary.

Phase III starts when the extraction of the remaining energy and angular momentum from the binary is mainly due to gravitational wave emission. At this point coalescence between the two black holes is inevitable.

The aim of this project is to investigate whether such systems are able to coalesce in less than the Hubble time. If so, such binaries would be a promising source for space gravitational wave detectors (such as the forthcoming LISA). However, the binary may stall at a separation of 1 parsec, generating the so called *Final Parsec Problem*, in other words the lack of low angular momentum stars able to interact with the binary. Recent studies have showed that the problem does not exist if one considers that the newly formed galaxy has a non negligible degree of axysymmetry and/or rotations, which lead to the presence of stars on centrophilic orbits that can interact with the binary.

The merger of the black hole binary will be studied, in this project, using a scheme proposed by Sesana and Khan able to reproduce accurate numerical simulations of colliding galaxies. For this purpose the binary host galaxy is modeled with a Dehnen profile and the time needed for the transition between *phase II* three-body encounters and gravitational wave emission is studied. The relation obtained is a function only of the stellar velocity dispersion and the galaxy density, evaluated at the influence radius of the binary. The results range from 0.1 to 10^2 Gyr. Since the Hubble time is of order of 13.7 Gyr, the coalescence not always occurs.

1.1 Outline of the project

The aim of this project is to analyze the mechanism that brings two massive black holes, each at the centre of the two galaxies that have experienced a merger episode, to coalescence, consequently emitting gravitational waves that can be detected.

In *Chapter 3* we provide observational evidence for the existence of black hole pairs in interacting galaxies.

In *Chapter 4* we give a detailed description of the phases of the evolution of the two black holes, following a galaxy merger.

In *Chapter 5* we discuss the *Final Parsec Problem* and its possible solutions.

In *Chapter 6* we set the galaxy characteristics for the calculations.

In *Chapter 7* we investigate the tight correlations between a black hole and its host galaxy.

In *Chapter 8* we estimate the time needed to reach the transition separation.

In *Chapter 9* we draw the conclusions to our work.

Chapter 2

Introducing black holes

Black holes, the most exotic prediction of General Relativity (GR), divide into two types according to their mass range: stellar and supermassive. There is also an intermediate class, which consists of black holes of intermediate mass, the so called "seeds", of which we do not have observational confirmation.

Solutions to the Einstein's field equations, in the context of General Relativity, have brought the idea of the existence of a singularity called black hole.

Black holes were viewed for much of the last century only as a mathematical curiosity. Only from 1963, with the discovery of extremely luminous distant objects called quasars, black holes began to be taken seriously. At the beginning they were associated only with the most energetic astrophysical contexts. The idea of supermassive black holes was proposed to explain the extreme luminosity of quasars, the most powerful sources of energy in the Universe, which were believed to be powered by accretion of gas and stars onto supermassive black holes. Later on, it became more and more clear that they are also present at the centres of galaxies, the bigger ones in bigger galaxies and the smaller ones in smaller galaxies. Their existence is, in fact, well established from measurements of velocities of gas and stars near the centre of nearby galaxies.

2.1 Black holes classification and interaction

Astrophysical black holes exist in two mass ranges:

- Stellar mass black holes that have masses up to $70M_{\odot}$, which are formed as the end product of stellar evolution of massive stars.
- Super massive black holes that are hosted at the centre of massive galaxies. Their masses range between $10^6 - 10^9 M_{\odot}$.

It is thought that black holes with mass ranging between $10^2 - 10^6 M_{\odot}$ exist. They are usually called *intermediate mass* or *middleweight black holes* and they are thought to be the seeds of formation of supermassive black holes, but haven't been observed yet.

It is currently thought that most massive black holes have formed through repeated episodes of accretion and by coalescence with other black holes as a consequence of galaxy mergers. The idea of black hole seed comes from here, but there are few theoretical constraints on the characteristics of such seeds. Therefore it is of great interest in astrophysics to disclose the mechanism of black hole seed formation through the detection of middleweight black holes in galaxies.

Moreover, tight correlations between the black hole mass M_{\bullet} and stellar velocity dispersion σ , ($M_{\bullet} - \sigma$ relation), and between M_{\bullet} and the stellar mass of the spheroid M_{*} , suggest that there is a process of symbiotic evolution between black holes and galaxies. Hence an understanding of the evolution of supermassive black holes can assist to understand the evolution of the galaxies.

In agreement with the current paradigm of hierarchical formation of galactic structures (Λ -CDM cosmology) galaxies are formed via hierarchical merging. The first objects that collapse under their own self-gravity are small halos that grow bigger through mergers with other halos and accretion of surrounding matter. This is a bottom up path, and the process is known as hierarchical clustering. Black holes form and evolve in the same bottom-up fashion. Black hole seeds themselves grow through galaxy mergers as we can see in *Figure 1*¹. Here are plotted tracks of black holes along cosmic history, in a mass versus redshift plane, as they experience accretion episodes and coalescence with other black holes. Coalescence episodes are marked with a circle.

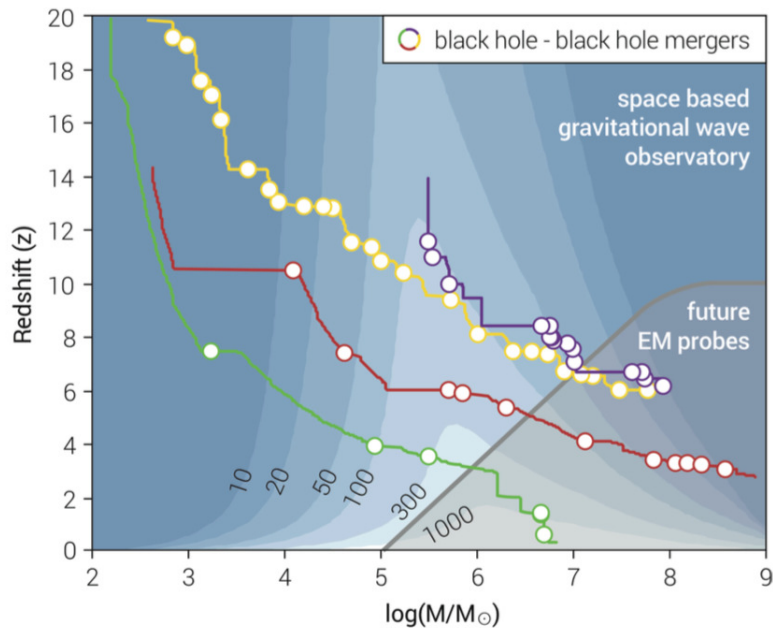


Figure 2.1: Plot of the evolution of black holes in a mass versus redshift plane

Four paths are reported: two ending with a black hole powering a $z \sim 6$ QSO (starting from a massive seed, blue curve), and from a seed resulting from the collapse of a massive

¹Figure from M. Colpi *Massive binary black holes in galactic nuclei and their path to coalescence*, 2014

metal-free star, yellow curve); a third ending with a typical $10^9 M_\odot$ black hole in a giant elliptical galaxy (red curve); and finally the fourth ending with the formation of a Milky Way-like black hole (green curve).

When two galaxies merge, each containing a black hole at its centre, the two black holes can eventually form a binary system in the merged galactic nucleus, inspiraling under the action of dynamical friction. Binary black holes thus appear as the inescapable outcome of galaxy assembly. When two massive black holes coalesce, they become one of the loudest sources of gravitational waves in the Universe.

2.2 Binary black holes merger rate and their detection

There are several interferometric ground based detectors for gravitational wave detection (such as LIGO, Virgo and GEO600) designed to observe neutron star or stellar-mass black hole binary coalescences in a frequency range from few Hz to few hundred Hz. Currently a space mission LISA (*Laser Interferometer Space Antenna*) is designed to measure gravitational waves for various sources over a range of frequencies between 0.03 mHz - 0.1 Hz. The prospect of the detection of low-frequency gravitational radiation by LISA has motivated theoretical studies into the formation and evolution of binary supermassive black holes. Such binaries would constitute the highest signal-to-noise ratio sources of low-frequency gravitational waves.

The event rate is still poorly known, with estimates ranging from a few to a few thousand events per year. A common practice when estimating event rates for LISA is to equate the binary SMBH coalescence rate with the galaxy merger rate, the latter derived from models of structure formation in which galaxies merge hierarchically.



Figure 2.2: Collision between two galaxies. Located 300 million light-years away in the constellation Coma Berenices, the colliding galaxies have been nicknamed "The Mice" because of the long tails of stars and gas emanating from each galaxy. Otherwise known as NGC 4676, the pair will eventually merge into a single giant galaxy.

Chapter 3

Observational evidence for interacting black holes

Observations of supermassive black hole pairs are either direct or indirect

According to hierarchical galaxy formation models, the formation of supermassive black holes binaries should be common in galaxies. The search for these binaries is of great interest for understanding galaxy formation and evolution. The detection of a supermassive black hole binary would strengthen the idea that black holes can grow to high masses in the centres of galaxies by merging with other black holes.

3.1 Direct observations

Here is a brief overview of some direct evidences which point to the presence of two supermassive black holes in the nucleus of a single galaxy.

- Starburst Galaxy NGC 6240



Figure 3.1: Optical (*left*) and X-ray (*right*) vision of the central region of NGC6240

NGC 6240 is a result of the merger of two galaxies and belongs to the ultra luminous infrared galaxy class. It harbors two optical nuclei. Due to the recent collision and merger of two galaxies the star formation rate is very high. Large amounts of gas and dust make it difficult to observe the central regions of the galaxy with optical telescopes. However, X-ray emissions from the central part of the galaxy can penetrate gas and dust. Observations performed with the Chandra X-ray observatory reveal the presence of two accreting supermassive black holes. The projected separation between the two black holes is 700 pc. Kinematic evidence suggest that the two supermassive black holes are not yet bound.

- **Spiral Galaxy NGC 3393**



Figure 3.2: Observational evidence for a supermassive black hole binary in the spiral galaxy NGC3393

A binary black hole system has been reported in the central regions of NGC 3393 after the observation of X-ray emission from the two AGNs, using NASA’s Chandra X-ray Observatory. Two two black holes are separated by ~ 135 pc and are estimated to have masses of $\sim 10^6 M_{\odot}$. NGC 3393 hosts the nearest known pair of supermassive black holes (at a distance of 160 million light years). It also happens to be the first time that a pair of supermassive black holes has been reported in a spiral galaxy like our Milky Way.

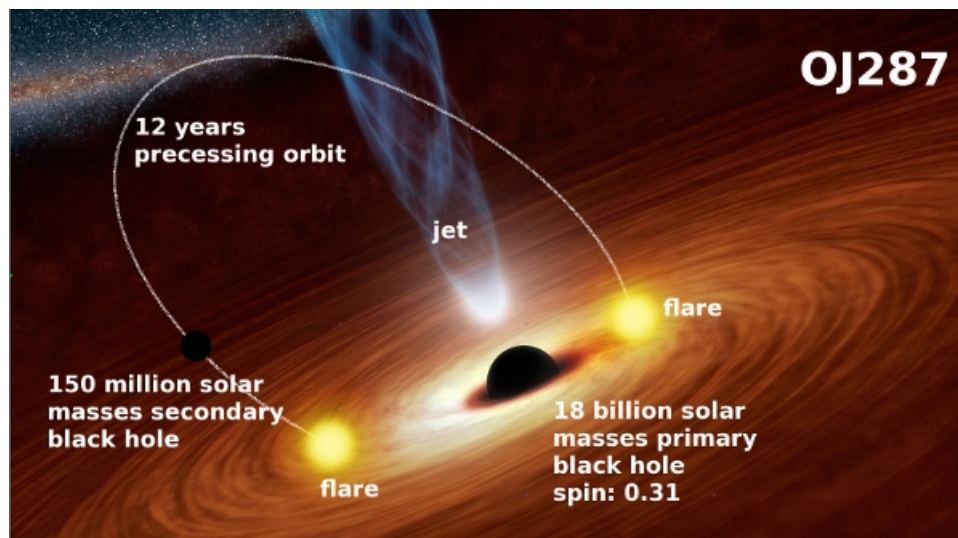
3.2 Indirect observations

The inspiral of a binary supermassive black hole binary is expected to leave a characteristic imprint in the morphological and dynamical properties of the newly formed galactic nucleus following the merger of two galaxies. Thus we provide some observed phenomena in galaxy centres that could be explained by different models of supermassive black binary evolution prior to or after the coalescence of the two black holes.

- **OJ 287**

It's one of the brightest quasars and it shows periodic outbursts in its light curve that have been observed since the late nineteenth century with a period of twelve years. There are various interpretations that involve the presence of a supermassive black hole binary:

- 1997: Katz proposed that the jet sweeps periodically across the line of sight as gravitational torque exerted by the secondary black hole causes precession of the accretion disk around the primary.
- 2008: Valtonen constructed the orbit of the black hole binary with eccentricity of 0.663. The mass of the primary is $18 \times 10^9 M_\odot$ and that of the secondary is about $10^7 M_\odot$. They also predicted the next outburst using the post Newtonian corrections to the binary orbit and observed the outburst to be in good agreement to their predictions.



- **SDSS J153636.22+044127.0**

Recently (2009), in a study by Boroson and Lauer, this quasar system has been proposed as a candidate for a subparsec supermassive black hole binary. The two black holes have masses $\sim 10^7 M_\odot$ and $10^9 M_\odot$. The binary separation is ~ 0.1 pc with an orbital period of ~ 100 years. The subparsec separation of the binary suggests that gravitational wave emission can drive the binary to coalescence in approximately 1 Gyr.

Chapter 4

Phases of coalescence

Binary black hole evolution consists of three distinct phases. The two black holes sink towards the centre due to dynamical friction until they form a bound pair, then slingshot ejection of stars remove energy and angular momentum from the binary until gravitational wave emission becomes the dominant mechanism in extracting the remaining energy and angular momentum. The two black holes can finally coalesce. However, it is not that simple as it is possible that it can take a time longer than the Hubble time.

Begelman et al., in an article published on *Nature* in 1980, pointed out three main steps along which coalescence proceeds:

- *Phase I: **pairing*** under dynamical friction in the stellar bulge after the merger until a Keplerian binary forms; the separation at this stage covers a range from 100 kpc down to ~ 0.1 pc.
- *Phase II: phase of **hardening*** during which the binary separation decreases as a consequence of energy and angular momentum loss by encounters with stars that cross the binary orbit; now the separation is reduced to $0.1 - 0.001$ pc.
- *Phase III: **gravitational wave** emission sets up and the binary finally coalesces.* The separation has gone below 0.001 pc.

Let's then analyze these phases one at a time.

4.1 Phase I

Dynamical friction causes orbital decay of satellite galaxies in the halo of larger galaxies. It is also responsible for star clusters and supermassive black holes sinking to the centres of galaxies. The cosmological growth of massive central black holes from minor and major mergers depends sensitively on dynamical friction. Dynamical friction can be seen as the drag induced on a massive body (satellite galaxy, star cluster, supermassive black hole, ...) by the stellar over-density raised by the massive body itself. Then it interacts with low velocity stars, slows and approaches the centre of the newly formed galaxy.

The principles of dynamical friction theory were formulated by Chandrasekhar in his work in 1943. Chandrasekhar assumed an infinite, homogeneous and isotropic background stellar distribution in which the massive body moves. The aim is that of the equipartition of the energy. All contributions to the dynamical friction force then come from the stars moving slower than the massive body. The singularity at large impact parameters is cut off by the use of a so-called Coulomb logarithm $\ln \Lambda$ which is the ratio of maximum to minimum impact factors.

Despite these simplifying assumptions, dynamical friction theory has worked remarkably well in a wide range of astrophysical situations since it was first formulated.

During *phase I* dynamical friction acts on each black hole until the separation is small enough for the Keplerian binary to form. Suppose to work in spherical symmetry. Dynamical friction is proportional to the background density of stars and to the square of the black hole mass.

$$\vec{F}_{df} \propto M_{\bullet}^2 \rho_* \ln \Lambda$$

where M_{\bullet} is the total mass of the binary

$$M_{\bullet} = M_{\bullet,1} + M_{\bullet,2}$$

If the N stars of the stellar background are described by a singular isothermal sphere, with density profile

$$\rho = \frac{\sigma^2}{2\pi G r^2}$$

and one-dimensional velocity dispersion σ , a black hole of mass M_{\bullet} at distance r sinks by dynamical friction on a timescale of

$$\tau_{df} \sim 2 \times 10^8 \ln^{-1} N \left(\frac{10^6 M_{\odot}}{M_{\bullet}} \right) \left(\frac{r}{100 \text{ pc}} \right) \left(\frac{\sigma}{100 \text{ km s}^{-1}} \right) \text{ yr} \quad (4.1)$$

The timescale decreases with decreasing distance from the galaxy's nucleus, so that dynamical friction becomes stronger as the orbit decays. The Keplerian binary forms when the mass in stars enclosed in the binary becomes comparable with the total mass of the binary

In a singular isothermal sphere a Keplerian binary forms when

$$a_{binary} \simeq \frac{GM_{\bullet}}{\sigma^2} \sim r_{inf}^1$$

that is a separation comparable with the gravitational sphere of influence of the black holes viewed as a single point mass M_{\bullet} . Dynamical friction guides the inspiral, without significant amplification of the eccentricity, down to a_{binary} .

¹See equation 8.1

Phase I ends when the binary separation has decayed below

$$a_{hard} = a_{binary} \frac{\mu}{3M_{\bullet}} \sim \frac{G\mu}{3\sigma^2} \sim 0.1 \frac{q}{(1+q)^2} \left(\frac{M_{\bullet}}{10^6 M_{\odot}} \right) \left(\frac{100 \text{ km s}^{-1}}{\sigma} \right)^2 \text{ pc} \quad (4.2)$$

where μ is the reduced mass of the binary

$$\mu = M_{\bullet} \frac{q}{(1+q)^2}$$

and q is the mass ratio defined as

$$q = \frac{M_{\bullet,2}}{M_{\bullet,1}} \leq 1$$

The hardening radius, a_{hard} , is defined as the binary separation at which the kinetic energy per unit mass of the binary equals the kinetic energy per unit mass of the stars in the galactic potential.

4.2 Phase II

During *phase II* the black hole binary loses orbital energy and angular momentum as a consequence of three-body encounters with single stars. A large number of stars is required to make a significant change in the binary binding energy.

The cross section of the binary is given by

$$A \sim \frac{\pi a G M_{\bullet}}{\sigma}$$

where a is the semi-major axis of the binary.

The corresponding hardening time is

$$\tau_{hard} \sim \frac{\sigma}{\pi G \rho a} \sim 70 \left(\frac{\sigma}{100 \text{ km s}^{-1}} \right) \left(\frac{10^6 M_{\odot} \text{ pc}^{-3}}{\rho} \right) \left(\frac{10^{-3} \text{ pc}}{a} \right) \text{ Myr} \quad (4.3)$$

where τ_{hard} increases as a decreases, because the cross section decreases with a . Thus a potential stalling of the binary can occur at the smallest binary separations.

4.3 Phase III

Phase III starts when the coalescence time driven by gravitational wave emission

$$\tau_{gw} \sim 5.4 \times 10^8 f(e)^{-1} \frac{q}{(1+q)^2} \frac{a^4}{M_{\bullet}^3} \left(\frac{1}{0.001 \text{ pc}} \right)^4 \left(\frac{10^6 M_{\odot}}{M_{\bullet}} \right)^3 \text{ yr} \quad (4.4)$$

drops below τ_{hard} , where

$$f(e) = \left[1 + \frac{73}{24}e^2 + \frac{37}{96}e^4 \right] (1 - e^2)^{-7/2}$$

is a function of the binary eccentricity.

The crossing condition, $\tau_{hard} = \tau_{gw}$, provides the binary separation at which the binary passes from *phase II* to *phase III*:

$$a_{II \rightarrow III} = \left(\frac{G^2}{c^5} \frac{256}{5\pi} \right)^{1/5} \left(\frac{\sigma}{\rho} \right)^{1/5} f^{1/5}(e) \left(\frac{q}{(1+q)^2} \right)^{1/5} M_{\bullet}^{1/5} \quad (4.5)$$

If τ_{gw} evaluated at $a_{II \rightarrow III}$ exceeds the age of the universe, then the binary stalls and does not reach coalescence. We can define a_{gw} as the separation at which the coalescence time τ_{gw} equals the Hubble time, τ_{Hubble} :

$$a_{gw} = 2 \times 10^{-3} f^{1/4}(e) \frac{q^{1/4}}{(1+q)^{1/2}} \left(\frac{M_{\bullet}}{10^6 M_{\odot}} \right)^{3/4} \left(\frac{\tau_{Hubble}}{13.6 \text{ Gyr}} \right)^{1/4} \text{ pc} \quad (4.6)$$

We can express it in terms of the Schwarzschild radius

$$r_S = \frac{2GM_{\bullet}}{c^2}$$

associated to $m_{\bullet,t}$ and for the case of equal mass circular binary

$$a_{gw} = 1.4 \times 10^4 \left(\frac{M_{\bullet}}{10^6 M_{\odot}} \right)^{-1/4} r_S$$

For a wide interval of stellar densities and velocity dispersions, the coalescence time τ_{gw} is less than the Hubble time, τ_{Hubble} , so the binary is expected to coalesce shortly after it has become hard. But the estimate of τ_{hard} underestimates the true hardening time since a large number of stars in "loss cone" orbits is necessary to drive the binary down to *phase III*. The loss cone is the domain, in phase-space, of stars with a sufficiently low angular momentum to interact with the binary. If the hardening occurs at a constant rate, the number of stars necessary to complete the hardening phase is comparable to the mass of the binary. In the case of massive black holes ($M_{\bullet} > 10^8 M_{\odot}$) such a large reservoir of stars may not be available.

The figure ² below summarizes the three phases: from the merging of the two galaxies, through interactions with single stars in three-body encounters til gravitational wave emission and coalescence. In particular it is a time versus black hole separation plot. We observe that the phase of interaction with low angular momentum stars (*phase II*) is the longest one.

²Figure from Khan *Dynamics and evolution of supermassive black holes in merging galaxies*, 2011

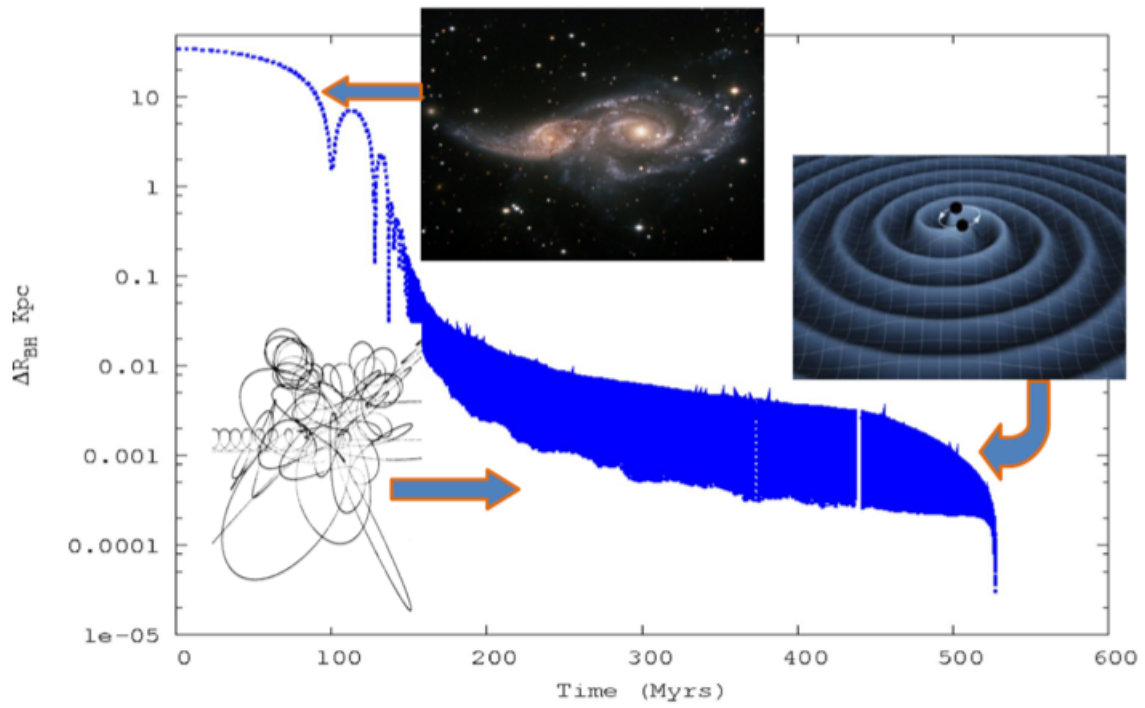


Figure 4.1: Different phases of two interacting supermassive black holes in a time versus binary separation plot. After the merger, dynamical friction works until a bound system forms, then the evolution is dominated by 3-body encounters with single stars and here we notice the variation of the separation due to the orbital period (the two bodies move from periastron to apastron). Finally gravitational wave emission brings to the inevitable coalescence.

Chapter 5

Final parsec problem

Final parsec problem and overcoming final parsec problem.

At the end of *phase I*, the black holes start ejecting stars from the loss cone at a high clearing rate. On the other hand, *phase II* needs a large reservoir of low angular momentum stars to interact with and lose additional energy and angular momentum in order to lessen the binary separation til orders of mpc are achieved.

Three body encounters take energy away from the binary. The refilling of stars in phase-space requires a lapse time comparable to the two-body relaxation timescale, which in galactic nuclei, viewed as spherical systems, is often longer than the Hubble time. Thus, the lack of stars in phase-space, causes the binary to stall, at a separation a_{stall} typically of $0.1 - 1$ pc, much larger than a_{gw} . The binary cannot reach coalescence in a Hubble time and this is referred to as *the last parsec problem*. The figure ¹ below summarizes the critical points.

Yu noticed that if we drop the assumption of sphericity, the hardening time, τ_{hard} , is lower and can be less than the Hubble time. Moreover, spherical galaxies have stars on centrophobic orbits, whereas galaxies with a higher degree of axisymmetry and triaxiality host a significant fraction of stars on centrophilic orbits, which can pass arbitrarily close to the binary and have low angular momentum. Real systems of merging galaxies present such degree of triaxiality or axisymmetry.

Direct N-body simulations confirmed that the end-product of a merger is not a spherical galaxy. The new galaxy retains substantial amount of asphericity or triaxiality such that the binary is seen to harden at a rate independent of N, as if the loss cone were fully refilled, or as if an N-independent mechanism provides a supply of stars in the loss cone orbits. Thus the last parsec problem appears to be an artefact of the oversimplifying assumption of sphericity of the relic galaxy.

¹Figure from Khan *Dynamics and evolution of supermassive black holes in merging galaxies*, 2011

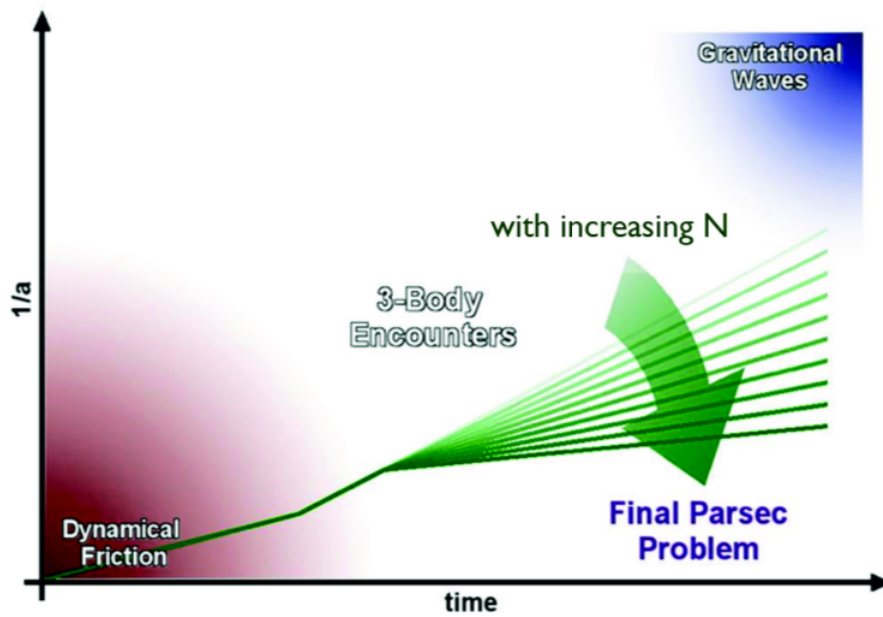


Figure 5.1: Scheme of the final parsec problem in a time versus $1/a$ plot: at the end of dynamical friction contribute, the binary is supposed to interact with single stars of the field in three-body encounters. These stars must have low angular momentum. If the star reservoir is not enough to extract the remaining energy and angular momentum from the binary and to shrink its separation to a distance of order of mpc, then the final parsec problem occurs, otherwise the binary enters the gravitational wave driven regime.

Chapter 6

Setting the galaxy model

In order to carry on some specific estimates of the time necessary for the binary to reach the transition separation, we need to set up a model for the galaxy. In this case we choose a spherical model (we do not reach the gravitational wave emission in our calculations, so we do not have to bother about the final parsec problem) represented by a Dehnen profile.

6.1 Dehnen profile

In isotropic spherical systems, the gravitational potential, Φ , and the density, ρ , depend only on one dimension, the distance r from the centre of the system. Spherical symmetry leads to $\rho(\vec{r}) \rightarrow \rho(r)$ and $\Phi(\vec{r}) \rightarrow \Phi(r)$. The gravitational potential and density are related through Poisson's equation

$$\nabla^2\Phi(r) = 4\pi G\rho(r)$$

This equation is paired with the Boltzmann equation for the equilibrium distribution function that gives the density profile for a galaxy.

In spherical symmetry Dehnen finds a possible solution characterized by a density profile:

$$\rho(r) = \frac{(3 - \gamma)M_*}{4\pi} \frac{r_0}{r^\gamma(r + r_0)^{4-\gamma}} \quad (6.1)$$

where M_* is the total mass of the galaxy, r_0 is the scale radius and γ is the inner logarithmic slope. We can rewrite it in terms of $x = r/r_0$, obtaining:

$$\rho(r) = \frac{(3 - \gamma)M_*}{4\pi} r_0^{-3} \frac{1}{x^\gamma(1 + x)^{4-\gamma}} \quad (6.2)$$

The scale radius r_0 is correlated with the effective radius as

$$r_0 = \frac{4}{3}(2^{1/(3-\gamma)} - 1)R_{eff} \text{ pc} \quad (6.3)$$

and the effective radius R_{eff} is defined as the radius at which the luminosity of the galaxy is half of the total luminosity (it is also called the *half light radius*).

γ is defined as the inner logarithmic slope

$$\gamma = \frac{d \ln(\rho)}{d \ln r}$$

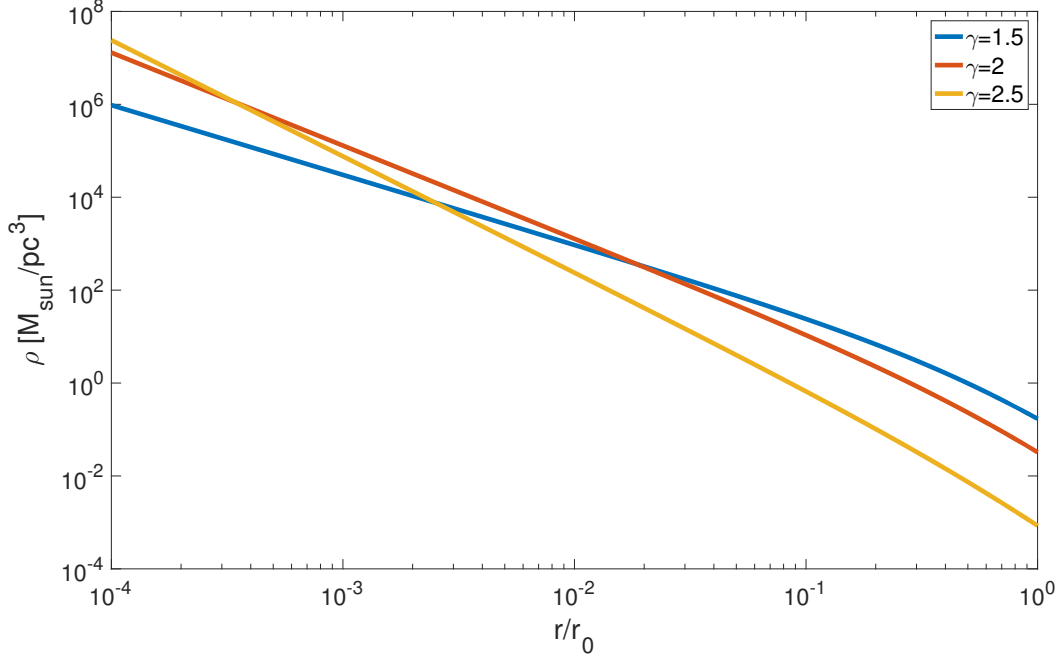


Figure 6.1: Dehnen density profiles for a fixed value of $M_* = 10^{10} M_\odot$, r_0 given by equation (6.3) and $R_{eff}(M_*)$ of order of some kpc

The bigger γ is the denser is the centre of the galaxy. The densities are proportional to r^{-4} at large radii and diverge in the centre as $r^{-\gamma}$ with $0 \leq \gamma < 3$. Thus this equation describes mass models with central density cusps that are shallower than r^{-3} or even asymptotically flat, with a divergence in the centre, as plotted above.

6.1.1 Circular velocity and velocity dispersion

The potential that corresponds to the Dehnen density profile is given by

$$\Phi(r) = \frac{GM_*}{r_0} \times \begin{cases} -\frac{1}{2-\gamma} \left[1 - \left(\frac{r}{r+r_0} \right)^{2-\gamma} \right], & \gamma \neq 2 \\ \ln \frac{r}{r+r_0}, & \gamma = 2 \end{cases} \quad (6.4)$$

Circular velocity, i.e. the velocity an object would have if it were revolving on a circular orbit around the centre at some distance r , can be calculated from

$$-\nabla\Phi = \frac{v_c^2}{r}$$

and is given by

$$v_c^2(r) = GM_* \frac{r^{2-\gamma}}{(r+r_0)^{3-\gamma}} \quad (6.5)$$

But the quantity that will be used in our forward calculations is the velocity dispersion. It is connected to the potential by the Jeans' equation and for the isotropic case the solution is

$$\sigma^2(r) = GM_* r^\gamma (r+r_0)^{4-\gamma} \int_r^\infty \frac{r'^{1-2\gamma}}{(r'+r_0)^{7-2\gamma}} dr' \quad (6.6)$$

At small radii

$$\sigma^2 \propto \begin{cases} r^{2-\gamma} & \text{for } \gamma \geq 1 \\ r^\gamma & \text{for } \gamma \leq 1 \end{cases}$$

Both v_c^2 and σ^2 diverge in the centre for model with $\gamma > 2$, they are finite for $\gamma = 2$ and decline to zero for $\gamma < 2$ (except for $\gamma = 0$ where $\sigma^2(0) = GM/30r_0$).

Here we plot velocities dispersions for different values of γ , using model units ($G = M_* = 1$).

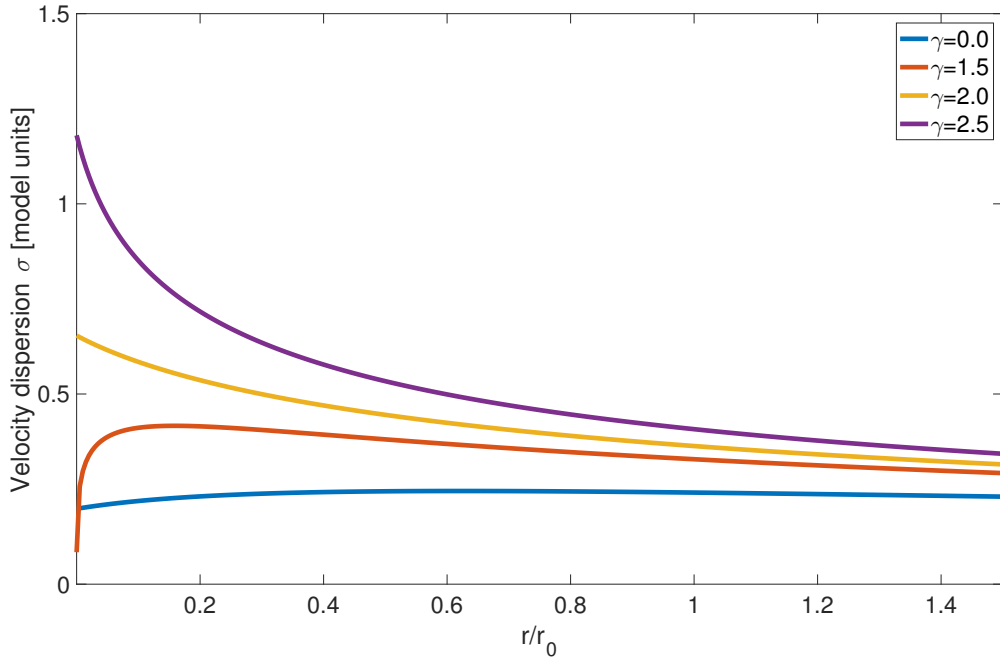


Figure 6.2: Velocity dispersion for different values of γ . Values of M_* and R_{eff} are as in *figure 6.1*

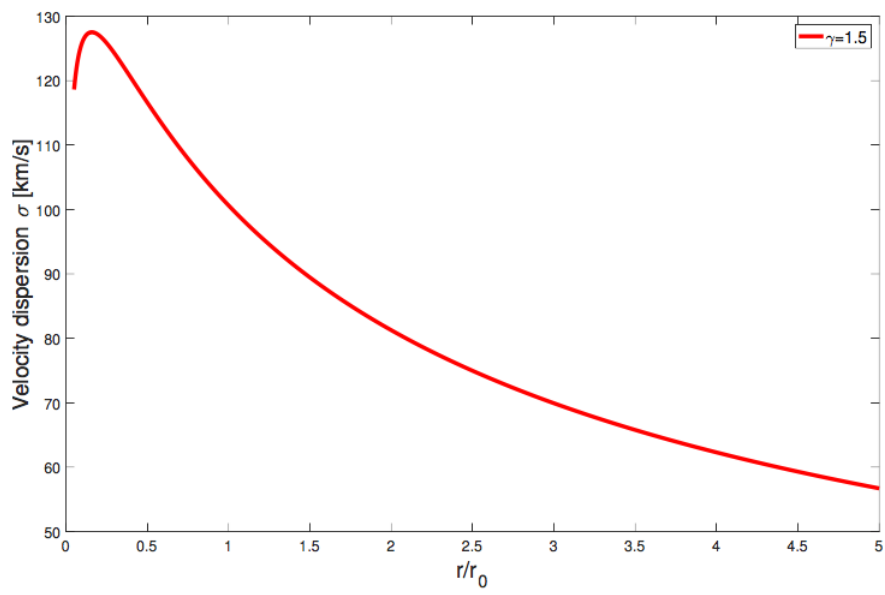


Figure 6.3: Velocity dispersion for a particular value of γ using an elliptic galaxy with mass of $M_* = 10^{10} M_\odot$.

Chapter 7

Black hole - host galaxy correlations

7.1 $M_{\bullet} - \sigma$ and $M_{\bullet} - M_*$ relations

The tight correlations between a black hole and its host galaxy take the form of the two famous $M_{\bullet} - \sigma$ and $M_{\bullet} - M_$ relations.*

The $M_{\bullet} - \sigma$ relation is an empirical correlation between the stellar velocity dispersion σ of the host galaxy, evaluated at far from the black hole sphere of influence, i.e. at a distance $r \sim r_0$ (see equation (6.3)), and the mass M_{\bullet} of the supermassive black hole at its centre.

Prior to the discovery of these relations, the main concern had been the simple detection of black holes, while afterwards the interest changed to understanding the role of supermassive black holes as a critical component of galaxies. This led to the main uses of the relation to estimate black hole masses in galaxies that are too distant for direct mass measurements to be made.

As reported by Kormendy and Ho (2013) this correlation is given by

$$\frac{M_{\bullet}}{10^9 M_{\odot}} = (0.310^{+0.037}_{-0.033}) \left(\frac{\sigma}{200 \text{ km s}^{-1}} \right)^{4.38 \pm 0.29} \quad (7.1)$$

The $M - \sigma$ relation would therefore imply a rough proportionality between black hole mass and bulge mass:

$$\frac{M_{\bullet}}{10^9 M_{\odot}} = (0.49^{+0.06}_{-0.05}) \left(\frac{M_*}{10^{11} M_{\odot}} \right)^{1.17 \pm 0.08} \quad (7.2)$$

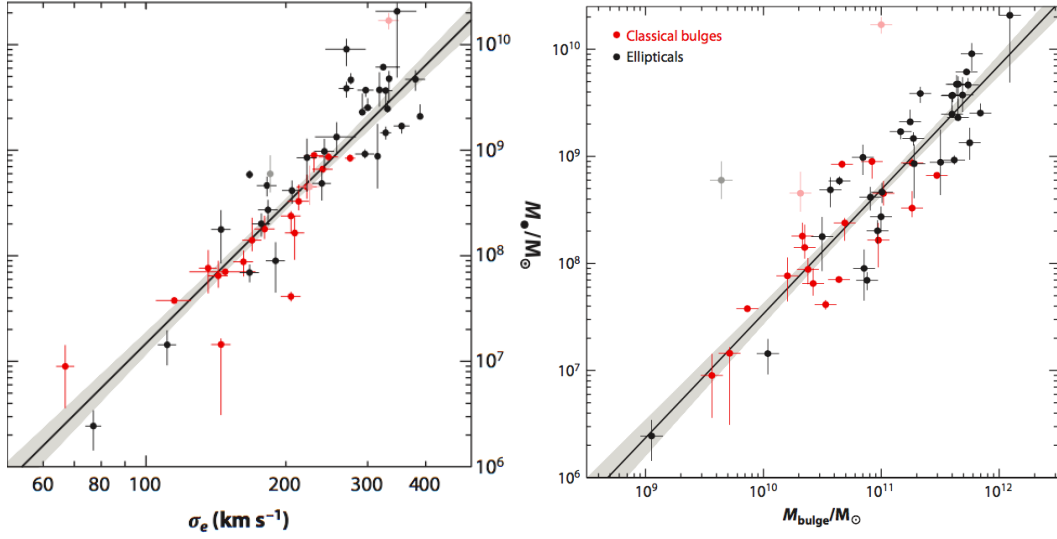


Figure 7.1: $M_\bullet - \sigma$ relation on the *left* and $M_\bullet - M_*$ relation on the *right*

7.2 Morphology of elliptic and spiral galaxies

The bifurcation observed in *figures* 8.2 and 8.3 reported in *section* 8.1 can be explained considering that the effective radius of galaxies depends on galaxy type and mass scale. In particular, the differentiation regards the ellipticals only. As we can see in the graphic below, more massive elliptic galaxies, with mass greater than $10^{11} - 10^{12} M_\odot$, follow the same pattern as the bulges of spirals, whereas those with lower masses follow a different one. Equations (8.5) and (8.6) confirm this.

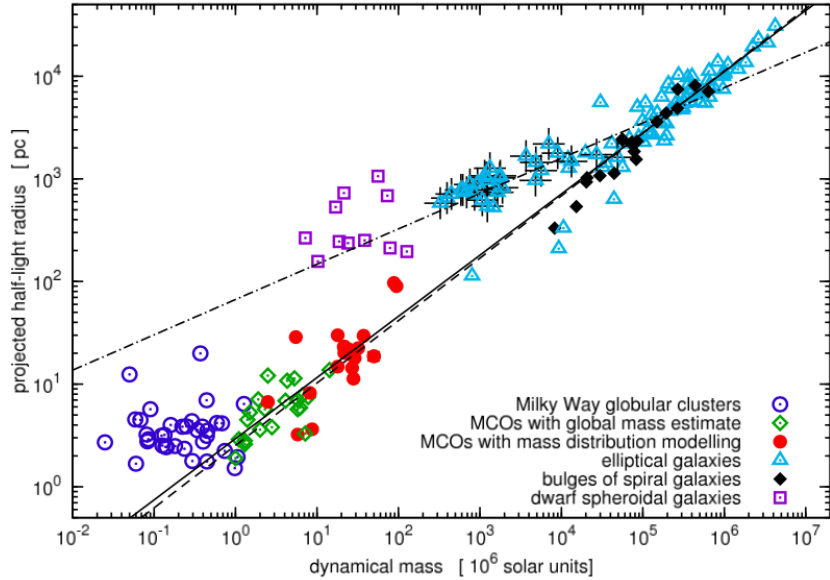


Figure 7.2: Plot of the effective radius R_{eff} against mass M

Chapter 8

Estimates of coalescence time

The massive black hole hardening rate is investigated following the work of Sesana and Khan (2015).

Sesana and Khan, in their recent work, suggested that the hardening time of a massive black hole binary, i.e. the rate at which the semimajor axis of the binary shrinks, is equivalent to that of a binary immersed in a field of unbound stars with density ρ_{inf} and velocity σ_{inf} , equal to the density and velocity dispersion of the surrounding stellar distribution at the binary influence radius. The influence radius, r_{inf} , is defined as the radius containing twice the binary mass in stars

$$M_*(< r_{inf}) = 2M \quad (8.1)$$

In their work, direct N-body simulations, made possible by parallel computing, were compared to an hybrid model based on 3-body scattering experiments. The results were that when the hybrid model was normalized to the stellar density and velocity dispersion at the binary influence radius, then the N-body hardening rate matched that predicted by 3-body scatterings. This result is particularly important since it allows to estimate a massive black hole binary lifetime on the only basis of the stellar density profile of the host galaxy.

We will explore the problem analyzing the two main contributions in *phase II* and *III*.

The evolution of the semi-major axis can be written as

$$\frac{da}{dt} = - \left. \frac{da}{dt} \right|_{3b} - \left. \frac{da}{dt} \right|_{gw} = -Aa^2 - \frac{B}{a^3} \quad (8.2)$$

where

$$A = \frac{GH\rho_{inf}}{\sigma_{inf}}, \quad B = \frac{64G^3 M_1 M_2 M f(e)}{5c^5}$$

G is the Newtonian gravitational constant, $G = 6.67 \times 10^{-8} \text{cm}^3 \text{g}^{-1} \text{s}^{-2}$

H is a constant that indicates a dimensionless rate ($H \sim 15$)

ρ_{inf} is the density at the influence radius

σ_{inf} is the velocity dispersion at the influence radius

M_1 and M_2 are the masses of the two black holes

$M = M_1 + M_2$

$f(e)$ is a function of eccentricity, already defined

c is the speed of light

Since the stellar hardening is $\propto a^2$ and the gravitational wave hardening is $\propto a^{-3}$, binaries spend most of their time at the transition separation given by imposing

$$\left. \frac{da}{dt} \right|_{3b} = \left. \frac{da}{dt} \right|_{gw}$$

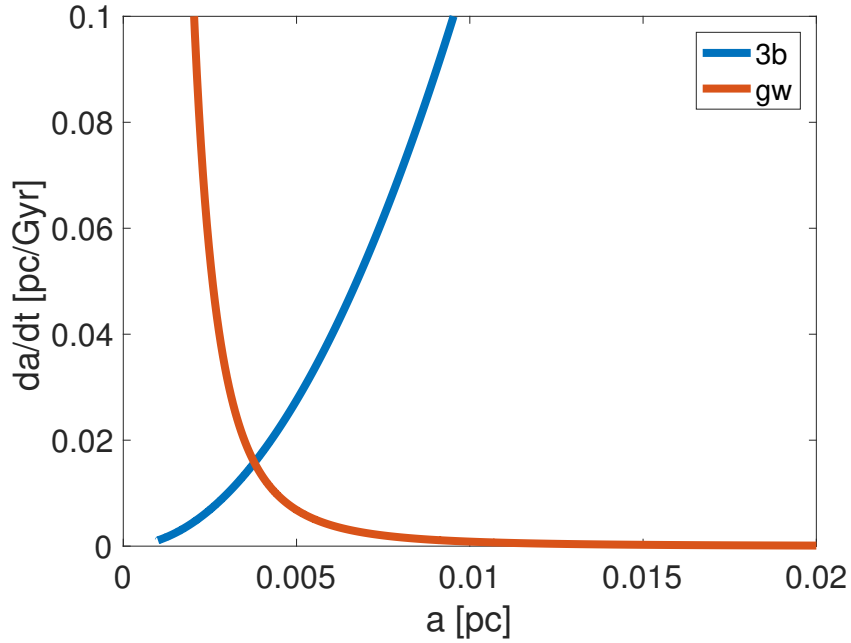


Figure 8.1: Plot of the two contributions to the semimajor axis shrinking

which gives

$$a_{*/gw} = \left[\frac{64G^2 \sigma_{inf} M_1 M_2 M f(e)}{5c^5 H \rho_{inf}} \right]^{1/5} \quad (8.3)$$

As a consequence, we can derive the binary lifetime integrating

$$\frac{da}{dt} \sim -Aa^2$$

Thus

$$t(a_{*/gw}) = \frac{\sigma_{inf}}{GH\rho_{inf}a_{*/gw}} \quad (8.4)$$

The lifetime estimated through this equation differs only about 10% from that obtained by integrating (8.1).

To get physical estimates for realistic galaxies we have to determine σ_{inf} and ρ_{inf} .

8.1 Plots of coalescence times

We plot equation (8.3) for different values of M_\bullet , ranging from 10^5 to $10^{11} M_\odot$. Given a fixed value of γ , for each value of M_\bullet we estimate the stellar mass from equation (7.2). Then we can calculate R_{eff} from the following relations

$$\frac{R_{eff}}{\text{pc}} = \max\left(2.95\left(\frac{M_*}{10^6 M_\odot}\right)^{0.596}, 34.8\left(\frac{M_*}{10^6 M_\odot}\right)^{0.399}\right), \quad \text{for elliptical galaxies} \quad (8.5)$$

$$\frac{R_{eff}}{\text{pc}} = 2.95\left(\frac{M_*}{10^6 M_\odot}\right)^{0.596}, \quad \text{for bulges of spirals and ultra compact dwarfs} \quad (8.6)$$

At this point the scale radius is given by

$$R_{eff} \sim 0.75r_0(2^{\frac{1}{3-\gamma}} - 1)^{-1} \quad (8.7)$$

and, finally, the influence radius is

$$r_{inf} = \frac{r_0}{\left(\frac{M_*}{2M}\right)^{\frac{1}{3-\gamma}} - 1} \quad (8.8)$$

For the σ estimate we use the equation (7.1).

We can make the following considerations:

- There is a bifurcation for masses lower than $\sim 10^9 M_\odot$ between elliptical galaxies and bulges of spiral galaxies. The dashed lines refer to the bulges of spirals, whereas the continuous ones to the elliptical galaxies. The reason why this occurs is explained in *section 7.2*.
- Varying the values of γ , (at fixed eccentricity and mass ratio), we observe that the binary lifetimes are longer for smaller γ as the density is lower and this leads to a longer $t_{a_{*/gw}} \propto \rho^{-1}$. In fact, the bulges of spirals, being denser than the ellipticals (see *section 8.2*), have, in general, minor binary lifetimes than the ellipticals. These times range from 0.1 to some tens of Gyr. On the other hand, the evolution of the semi-major axis is nearly the same for different values of γ .

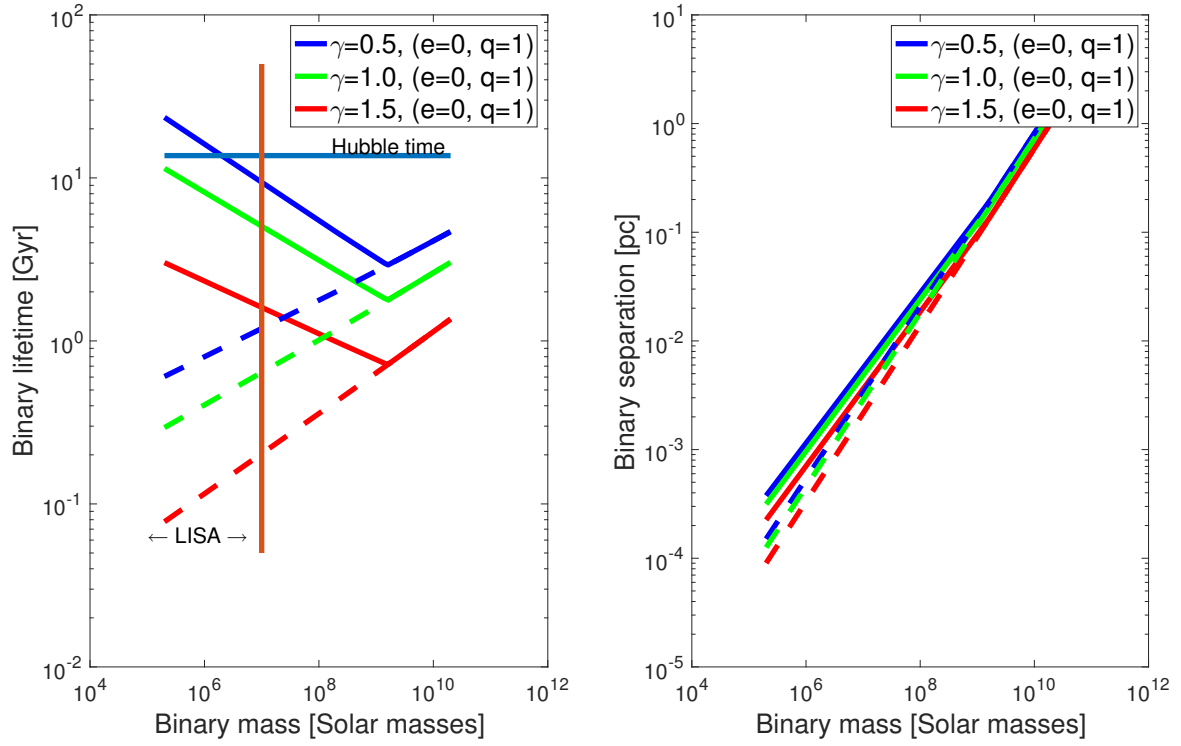


Figure 8.2: Binary lifetime and separation for varying γ .

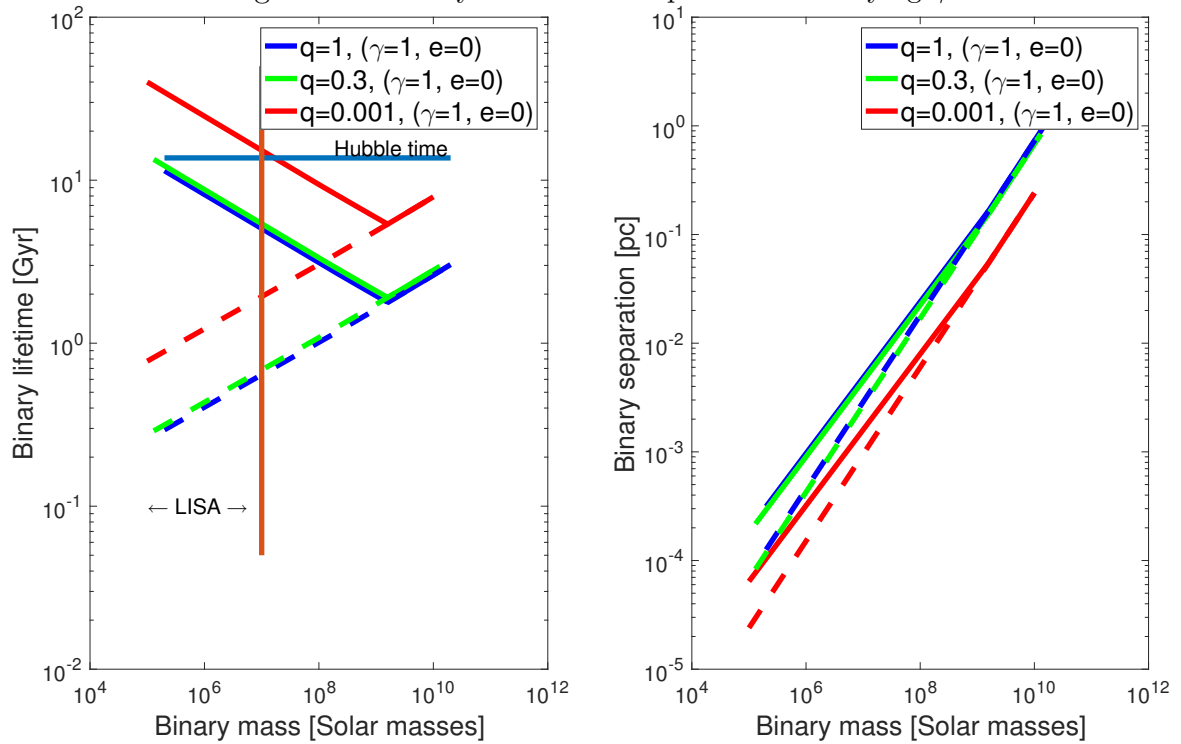


Figure 8.3: Binary lifetime and separation for varying q .

- If we vary the values of the binary mass ratio, at fixed γ and eccentricity, we observe that the times are smaller for equal mass black holes, differing by an order of magnitude from those relative to smaller mass where q varies between 1 and 0.001.
- The Milky Way is a spiral galaxy hosting a black hole of $4 \times 10^6 M_\odot$, named *Sgr A**, and surrounded by a bulge of $4 \times 10^9 M_\odot$. It is fated to merge with the Andromeda galaxy in about 4 Gyr. Also Andromeda hosts a black hole of comparable mass as that of *Sgr A**. Our model predicts that the hardening phase of the two black holes, when the merger is completed will occur in a timescale less than 1 Gyr. For the case of dwarf galaxies the time scale can be much longer.
- The forthcoming LISA project will be able to detect coalescing binaries in the mass range from $10^4 M_\odot$ to $10^7 M_\odot$.

8.2 Stellar density in elliptical galaxies and in bulges of spirals

The table gives the values of the stellar densities of elliptical galaxies and bulges of spiral galaxies against the central black hole binary mass, extrapolated from the calculations, done below, for the estimates of coalescence time.

$M_{tot,\bullet}$ [$M_\odot \times 10^6$]	$\rho_{elliptic}$ [N/pc^3]	ρ_{bulge} [$N/pc^3 \times 10^3$]
0.2	119.1	11.6
0.6	89.85	4.98
1.2	75.16	2.93
1.6	69.78	2.35
2.2	64.26	1.84
3.0	59.29	1.45
4.2	54.33	1.12
5.4	50.89	0.92
6.6	48.30	0.79
7.8	46.24	0.69
9.2	44.29	0.61
11	42.27	0.53
14	39.68	0.44
16.8	37.83	0.38
19.2	36.53	0.35
20	36.14	0.34

In the graphics below we plot the black hole binary mass against the density of the merging galaxies, both for ellipticals and bulges of spirals, and we observe that

- In the case of ellipticals the mass to consider is the whole mass of the galaxy, whereas for spirals only the mass of the bulge has a role;

- Stellar density in the bulges of spiral galaxies is about two orders of magnitude greater than that of elliptical galaxies.

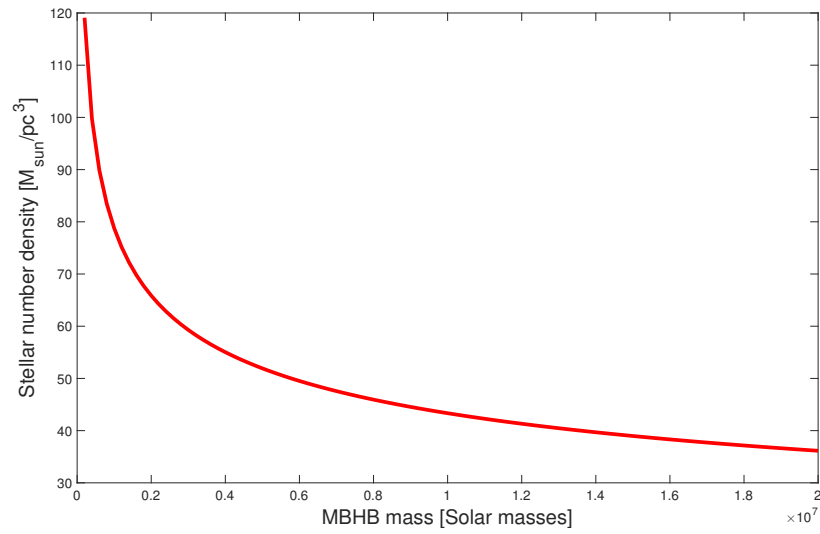


Figure 8.4: Stellar density in elliptical galaxies, with $M_* = 10^{11}M_{\odot}$ and R_{eff} as calculated from equation (8.8)

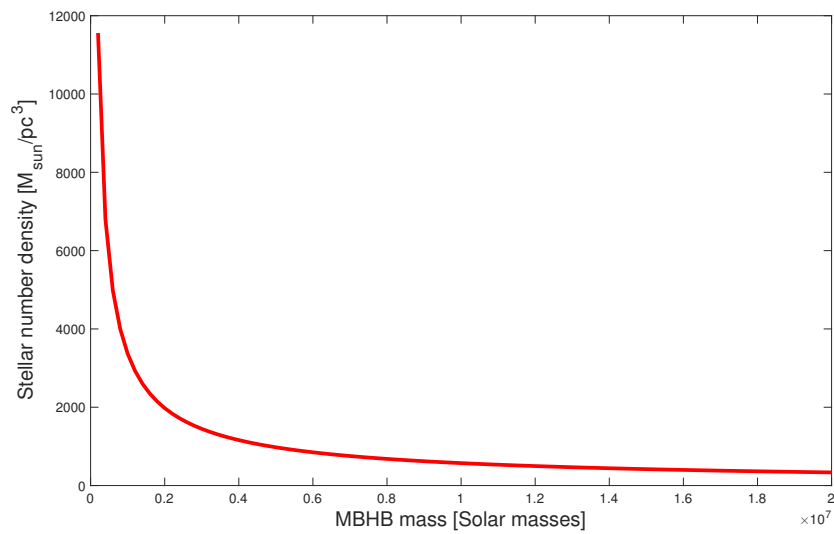


Figure 8.5: Stellar density in bulges of spiral galaxies, with $M_* = 10^{10}M_{\odot}$ and R_{eff} as calculated from equation (8.9)

Chapter 9

Conclusions

Binary black holes can reach coalescence following the emission of gravitational waves. But the conditions under which this could happen are that the two black holes have to be driven to separation minor than 0.001 pc, for the gravity is a weak force and gravitational waves are a result of strong field regimes. This is a very small distance if we compare it to a galaxy size and merging galaxies are where these events take place. There are mechanisms that allow to extract energy and angular momentum from the binary, but it is not certain that the coalescence will be reached. The process is long and complex.

Three phases characterize the process, from a phase of pairing under dynamical friction until a Keplerian binary is formed, through a phase of hardening with interactions with single stars to a final phase of inspiral driven by gravitational wave emission. If the system presents a spherical symmetry than the final parsec problem can occur. But, thanks to recent simulations it has been confirmed that the final parsec problem arises only because of oversimplification of the models. In fact, galaxies, after the merger, are not spherical systems, but present a certain degree of triaxiality or axisymmetry.

The problem of coalescence is still open and nowadays estimates of coalescence times range between several Myr to several Gyr.

Acknowledgements

This project came out to be more challenging than expected, but ended up with quite a satisfying result. Some people supported me during the work and I'd like to thank them.

I thank my supervisor, Monica Colpi, who gave me all the suggestions and corrections, helping me to understand the most critical points.

I thank Luca Prudenzi, who encouraged me and gave me his support through the whole writing.

I thank my mum and my sister who indirectly stood for me all the time.

Bibliography

- [1] M. Stenmetz, E. Müller *Formation of spiral and elliptical galaxies in a CDM cosmogony*, 1993.
- [2] W. Dehnen *A family of potential-density pairs for spherical galaxies and bulges*, 1993
- [3] L. Ferrarese, D. Merrit *A fundamental relation between supermassive black holes and their host galaxies*, 2000.
- [4] A. Marconi, L. Hunt *The relation between black hole mass, bulge mass, and near infrared luminosity*, 2003.
- [5] N. Häring, H-W Rix *On the black hole mass - mass bulge relation*, 2004
- [6] L. Ferrarese, H. Ford *Supermassive black holes in galactic nuclei: past, present and future research*, 2004.
- [7] D. Merrit, M. Milosavljević *Massive black hole binary evolution*, 2005.
- [8] F. Pretorius *Binary black hole coalescence*, 2007.
- [9] J. Dabringhausen, M. Hilker, P. Kroupa *From star cluster to dwarf galaxies: the properties of dynamically hot stellar systems*, 2008.
- [10] Khan et al. *Efficient merger of binary supermassive black holes in merging galaxies*, 2011.
- [11] Khan *Dynamics and evolution of supermassive black holes in merging galaxies*, 2011.
- [12] Khan et al. *Merger of unequal mass galaxies: supermassive black hole binary evolution and structure of merger remnants*, 2012.
- [13] Seoane et al. *Doing science with eLISA: astrophysics and cosmology in the millihertz regime*, 2012.
- [14] J. Kormendy, L. Ho *Coevolution (or not) of supermassive black holes and host galaxies*, 2013.
- [15] M. Colpi *Massive binary black holes in galactic nuclei and their path to coalescence*, 2014.
- [16] Kovetz et al. *The black hole mass function from gravitational wave measurements*, 2016.

[17] D.Merritt *Dynamics and evolution of galactic nuclei.*